

Research Article

Study on Internal Vibration Law and Vibration Reduction of Xiaoxiku Tunnel Blasting

Sheng-Lin Li, Shu-Feng Liang , and Jia-Wei Lu

School of Mechanics & Civil Engineering, China University of Mining & Technology, Beijing, China

Correspondence should be addressed to Shu-Feng Liang; 201638@cumtb.edu.cn

Received 18 February 2022; Accepted 2 April 2022; Published 25 April 2022

Academic Editor: Zhongguang Sun

Copyright © 2022 Sheng-Lin Li et al. This is an open access article distributed under the Creative Commons Attribution License, which permits unrestricted use, distribution, and reproduction in any medium, provided the original work is properly cited.

Efficient and economical drilling and blasting method is widely used in tunnel excavation projects, but the vibration problem caused cannot be ignored. The blasting vibration in the near area directly damages the surrounding rock and supporting structure, and the vibration in the middle and far area affects the stability of the surrounding rock, the primary support, and even the secondary lining. Based on the blasting excavation of Xiaoxiku tunnel, blasting vibration tests were carried out. In addition, the measured data were analyzed by using nonlinear regression and Fourier transform of Sadowski formula. According to the interference vibration reduction method, the blasting vibration of group holes is analyzed, and the results provide a reference for blasting design optimization of Xiaoxiku tunnel or similar soft rock tunnel. The results showed that the blasting vibration test data showed that the peak vibration velocity generated by the blasting of cut hole is the largest. Based on the measured vibration waveform of single-hole blasting, MATLAB software is used to carry out superposition operation, so as to determine the best delay time of single-hole continuous blasting vibration reduction, and the value is calculated as 7 ms. According to the superposition operation results, the experiments of the cut area under different delay intervals were carried out. The measurement vibration waveform showed that the peak vibration velocity is the minimum when the delay interval is 7 ms. The actual measurement results are the same as the calculation results. The measured blasting waveform distribution is relatively uniform, and the vibration duration is moderate. The vibration speed decreases, while the main frequency increases.

1. Introduction

The drilling-blasting method is a construction method for tunnel excavation projects which appeared in the 1960s with the invention of yellow explosives and the birth of the first air-driven rock drill. This construction method has the characteristics of high efficiency and strong controllability, which is especially suitable for the excavation of mountain tunnels with complex and changeable terrain. Besides, it also has the advantages of saving construction costs and less energy consumption; thus, it has been widely used in engineering in decades of years. Unfortunately, the drilling-blasting construction method has many inherent shortcomings. For example, part of the energy generated by the explosive will propagate to the surroundings in the form of waves, which will cause the vibration of the tunnel body. This phenomenon is called the blasting vibration effect [1]. Moreover,

many unfavorable geological conditions such as soft rocks and faults may be encountered during the construction of the tunnel. Such engineering geological conditions have a stronger response to blasting vibration, and the structural problems induced by vibration damage will be more prominent. Under such working conditions, the safety of tunnel blasting should be paid more attention [2–4].

When evaluating the influence of tunnel blasting vibration on tunnel safety, it is necessary to calculate the safety factor based on frequently used theories, obtain reliable test data through the means of experiment, and then achieve precise control of blasting vibration on-site construction and protection of the safety of the tunnel itself and surrounding structures.

In this paper, the blasting construction of the Xiaoxiku tunnel in the Xitong Road (Hebei Road-Miguan Road) project in Miyun District is taken as the background, and a

combination of theoretical research and field tests is used to study the influence of blasting vibration on the surrounding rock in the tunnel. Also, a suitable blasting vibration reduction plan is proposed, which has very important practical significance for the safety of the surrounding rock and supporting structure in the tunnel blasting of this project [5, 6].

In current studies, the attenuation of tunnel blasting vibration was mainly focused on its cavity effect on the tunnel excavation faces in front and behind the tunnel working face and the blasting vibration of adjacent tunnels [7–10], but the vibration attenuation inside the tunnel is more important for the tunnel safety, which should be paid enough attention. There were a few studies that have been conducted on the internal vibration law of tunnel blasting. Fu et al. [11] arranged the measuring points on the vault and sidewall of the adjacent roadway working face and used these measuring points to obtain the vibration of the lateral surrounding rock and directly above the roadway working face. Results showed that the vibration velocity of the arch foot and sidewall in the section parallel to the tunnel face is less than the vibration velocity of the vault particle.

In order to effectively control the effect of blasting vibration and reduce its damage to surrounding buildings (structures) or its own structure, researchers have carried out a large number of studies on vibration speed control methods. The means of vibration has become a hot issue of vibration reduction in recent years [11–15].

For the purpose of vibration reduction, different viewpoints have been put forward on determining a reasonable millisecond time [16–19]. Yang et al. [20–22] conducted a detailed and in-depth study on the millisecond interference vibration reduction method by using numerical analysis method and obtained initiation vibration of different sections of charge after stacking vibration waveform under different delay time. The intensity is relatively weak; if $n > 3$, the vibration waves generated by the explosion of each charge are separated from each other and do not interfere with each other. Because the delay error of the detonator is large and it is difficult to obtain the superimposed vibration wave in advance, also the results obtained by using different calculation methods under the same blasting conditions have large scatters, and the ordinary interference vibration reduction method calculated by the theory is difficult to be used in practical applications.

By analyzing the measured blasting vibration signals, an interference suppression law can be obtained. By analyzing the differences of subsignals, segmented vibration waves (or subsignals) can be separated from the recorded millisecond blasting vibration signals. The superimposition effect under the delay time is used to select the appropriate micro-difference delay time, through which the purpose of interference and vibration reduction can be achieved, and the active control of blasting vibration disasters can be realized. In order to determine the best delay time for electronic detonators, Gong et al. [22] analyzed the tunnel blasting vibration waveform through MATLAB programming and found that when the delay time is at 0.4 to 0.7 times, 1.4 to 1.7 times, and 2.4 to 2.7 times of the main period, the peak

vibration speed of the waveform is the smallest, and it also verified the feasibility of staggered vibration reduction. Besides, in the study of Fu et al. [23], in order to reduce the vibration of tunnel blasting, the use of electronic detonators can realize the principle of interference and vibration reduction caused by single-hole blasting. Through experiments, it was found that the vibration generated by electronic detonator blasting is 70% lower than that generated by nonel detonator.

Based on the theory of interference vibration reduction, this paper takes the blasting construction of Xiaoxiku tunnel in Xitong Road project in Miyun District as the background, uses the method of combining theoretical research and field test to study the influence of three-step blasting vibration on the surrounding rock in the tunnel, and puts forward a suitable blasting vibration reduction scheme to ensure the safety of tunnel structures.

2. Vibration Test of Xiaoxiku Tunnel Blasting Construction Site

2.1. Project Overview. The Xiaoxiku tunnel is a separated tunnel with a total length of 1247 m of medium-sized. The starting and ending length of the tunnel on the left is ZK12+948~ZK13+505, with a total length of 557 m, and the starting and ending length of the tunnel on the right is YK12+880~YK13+490, with a total length of 690 m. The section size of the tunnel is 14.1 m in width and 11 m in clear height. The entrance section and exit section at both ends of the tunnel are open tunnels, and the rest are concealed tunnels. The design and construction of the tunnel adopted the principle of the new Austrian method, and the initial support was composed of bolts, steel mesh, sprayed concrete, and steel arches. The secondary lining was made of reinforced concrete and molded concrete, which together form a permanent bearing structure. The tunnel is located in low mountains and hilly areas, dominated by bedrock strata, which is mainly the bedrock of the Wumishan Formation of the Jixian System of the Upper Proterozoic. The stratum contains siliceous band fine-crystalline dolomite, stromatolite silt-crystalline dolomite, and siliceous belt laminar fine-crystalline dolomite. The rock mass is layered structure with well-developed joints. The weathering of the rock is affected by topography, lithology, and structure. The surrounding rock is class v.

2.2. Excavation and Blasting Scheme. The tunnel excavation adopted the three-step seven-step excavation method. After several tested explosions during the early construction process, it was found that when the reserved core soil of the upper step exists, the rock clamps of surrounding face rock mass will rise. The existence of core soil results in poor blasting effect. At the same time, considering that the increase in the number of blasting holes and the amount of charge will increase the cycle time and cost of the construction period, the blasting with a larger charge will often have a higher damage risk. Therefore, the blasting plan was improved in the later construction process: the core soil of the upper step was removed, and the charging face created by the core soil

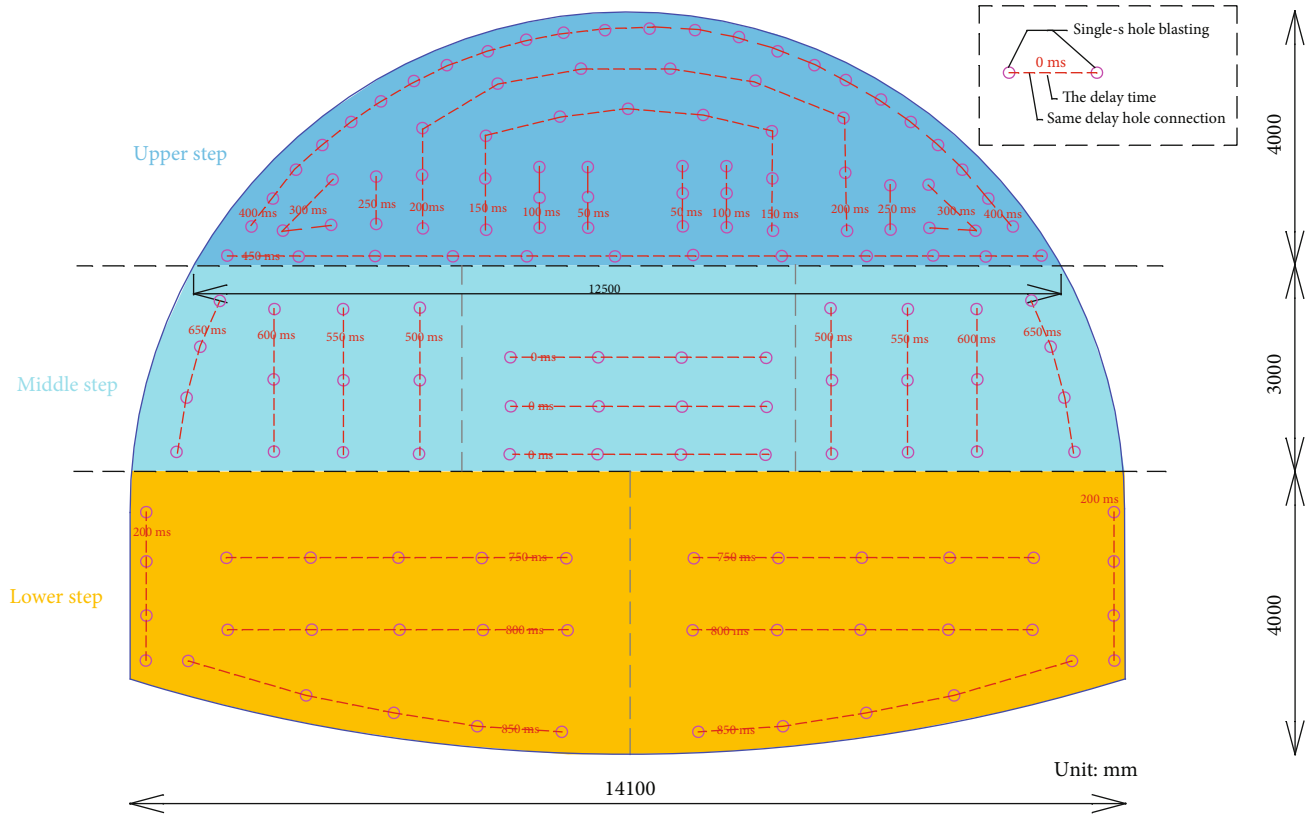


FIGURE 1: Holes layout and initiation sequence diagram of three-step all-in-one blasting.

of the upper step was replaced by a bench. The stability of the surrounding rock of the face can also meet the requirements when there is no core soil.

The tunnel face is blasted at the same time with the upper, middle, and lower steps. No delay time is set between the holes of each section of the tunnel face, and the delay time between each section is set to be 50 ms. A 50-ms delay interval is adopted between the upper step cut hole, auxiliary hole, and caving hole section, and no delay is set between holes. The cut hole time is set to be 50 ms, the auxiliary hole delay time is 100 ms, and each section of blastholes increases by 50 ms sequentially. The middle step adopts the blasting scheme of the row of guns. The initiation time of the first row of blastholes is set to be 50 ms. After that, each row of blastholes is delayed by 50 ms, and there is no delay interval between each row of holes. The lower step adopts the same delay setting as the middle step. Therefore, in each blasting work, the three steps are detonated at the same time, and the measured blasting vibration waves generated between the three blasting sources are superimposed. The arrangement of the three-step blastholes and the detonation sequence are shown in Figure 1.

TC-4850 blasting vibrometer is used in the field blasting test acquisition system. The sampling frequency of the vibrometer is 1 K~50 KHz, the frequency response range is 5 Hz~500 Hz, and the recording accuracy is 0.01 cm/s. TCS-B3 low-frequency broadband three-dimensional vibration velocity sensor is adopted to monitor blasting vibration.

3. Study on Vibration Law of Xiaoxiku Tunnel Blasting

3.1. *Layout of Tunnel Vibration Measuring Points.* Three vibration measuring instruments are arranged in the tunnel, and the measuring points are arranged in sequence along the center line of the tunnel. In the experiment, three measuring points are set at 40 m, 45 m, and 50 m away from the excavation face. Keeping the positions of the measuring point unchanged, the vibration waveforms of the measuring points are recorded with the increase of the depth of the excavation face. Due to the proximity of the tunnel face, the collector is placed in a steel cage to protect the instrument. The layout of measuring points is shown in Figure 2.

3.2. *Results of Vibration Monitoring Data.* On the tunnel measurement points, a total of 21 sets of the vibration data were obtained. According to previous studies, in the cut hole blasting, the maximum value of the vibration speed may be occurred by the clamping of the cut hole. Therefore, the blasting of cut hole and surrounding hole is mainly studied.

3.2.1. *Permission to Reuse and Copyright.* The vibration data of 21 groups of cut blasting were counted, and the results were shown in Table 1.

3.2.2. *Analysis of Typical Waveforms of Vibration at Measuring Points.* The waveforms at the tunnel measurement points when the three steps blasted at the same time are collected, at a distance of 75 m from the upper step, as



FIGURE 2: Layout of bottom plate measuring points.

shown in Figure 3. The total charge for the blasting operation is 204 kg. It can be clearly seen from the figure that the vibration waveform has apparent multisegment characteristics. Since the delay time between the three-step initiation network segments is set as 50 ms, the response on the waveform graph shows that the time difference between each peak is about 50 ms, where the first wave peak has a larger value, and the wave peak is the superimposed effect of the Cut notch blasting of upper step and blasting of the first section of middle and lower step. The effect of step cut hole blasting and the first stage blasting of the middle and lower steps is superimposed. As the cut blasting has the greatest clamping effect, the superposition causes a larger vibration peak. After that, the three steps will sound once every 50 ms. The vibration waveform generated by the whole blasting operation approximately lasts for 0.5 s.

According to Figure 3, the whole process of vibration at the measuring point of upper bench blasting lasts about 500 ms. The particle vibration velocity caused by cutting blasting is the largest, and the clamping effect is the largest at this time. Therefore, the clamping effect is an important factor affecting the vibration intensity. Because the free surface is produced after the blasting in the cut area, and the single-stage charge is reduced compared with the cutting

charge, the amplitude of the subsequent caving hole blasting decreases and lasts for a long time, showing a multistage continuous waveform. The blasting of the peripheral hole has sufficient free surface, but the single-stage charge of the peripheral hole is the largest, resulting in a higher peak vibration velocity than that of the caving hole. Therefore, the charge is another important factor affecting the blasting vibration intensity.

3.3. Research on Law of Vibration Velocity Attenuation

3.3.1. *Nonlinear Regression Method of Sadowski's Formula.* In the vibration velocity regression analysis, the Sadowski formula is used, as shown in Equation (1)

$$V = K \cdot (Q^{1/3}/R)^\alpha, \quad (1)$$

where V —particle peak vibration speed (cm/s) Q —amount of explosive (Kg) R —distance between blasting center and monitoring position (m) K, α —parameters related to topography and geological conditions

The calculation process of Sadowski's formula by using nonlinear regression method is as follows:

TABLE 1: Monitoring data of the particle vibration velocity of the cut hole.

Serial number	Distance (m)	Explosive charge Q (kg)	Explosive charge in cut hole Q (kg)	Maximum vibration speed Vmax (cm/s)		
				Horizontal radial direction	Horizontal tangential direction	Vertical direction
1	40			1.23	1.25	1.93
2	45	156	11.8	0.98	0.82	1.82
3	50			0.87	0.94	1.45
4	42.1			1.02	1.21	1.7
5	47.1	162	12.6	0.98	0.87	1.39
6	52.1			0.68	0.81	1.24
7	44.1			1.12	1.13	1.76
8	49.1	156	12.8	0.74	0.75	1.35
9	54.1			0.8	0.83	1.29
10	46.3			0.86	0.87	1.48
11	51.3	132	10.8	0.68	0.68	1.34
12	56.3			0.55	0.73	1.16
13	48.1			0.88	0.89	1.58
14	53.1	144	12.4	0.56	0.68	1.08
15	58.1			0.64	0.54	0.88
16	52.3			0.83	0.78	1.11
17	57.3	162	12.6	0.67	0.69	1.01
18	62.3			0.47	0.58	0.87
19	54.6			0.85	0.73	1.07
20	59.6	162	12.6	0.58	0.70	1.08
21	64.6			0.59	0.53	0.97

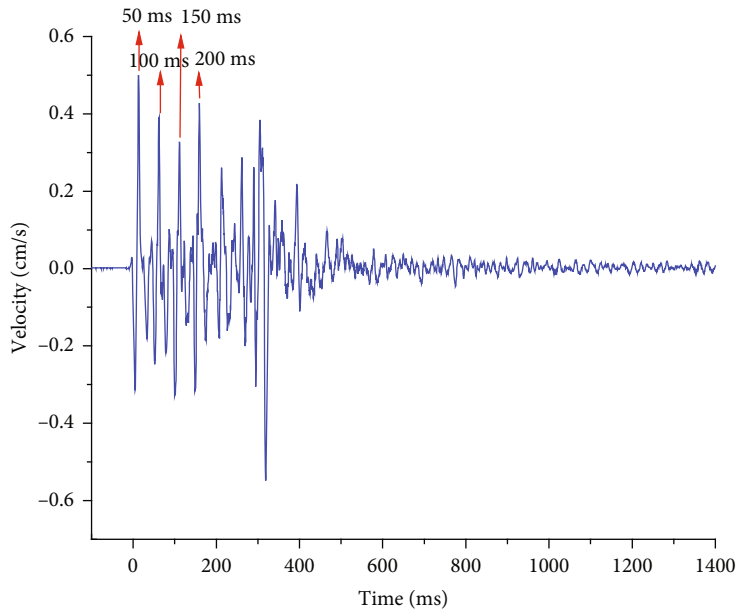


FIGURE 3: Typical waveform produced by three explosion sources.

According to the limit theorem of the binary function, when the nonlinear residual square sum M^2 takes the minimum value

$$\left. \begin{aligned} \frac{\partial M^2}{\partial K} &= 0 \\ \frac{\partial M^2}{\partial \alpha} &= 0 \end{aligned} \right\}, \quad (2)$$

$$M^2 = \sum_{i=1}^n (V_i - K\rho_i^\alpha)^2. \quad (3)$$

Expand the above formula to get

$$\left. \begin{aligned} \sum_{i=1}^n (V_i - K\rho_i^\alpha)\rho_i^\alpha &= 0 \\ \sum_{i=1}^n (V_i - K\rho_i^\alpha)\rho_i^\alpha \ln \rho_i &= 0 \end{aligned} \right\}, \quad (4)$$

$$\left. \begin{aligned} \sum_{i=1}^n V_i \rho_i^\alpha &= K \sum_{i=1}^n \rho_i^{2\alpha} \\ \sum_{i=1}^n V_i \rho_i^\alpha \ln \rho_i &= K \sum_{i=1}^n \rho_i^{2\alpha} \ln \rho_i \end{aligned} \right\}. \quad (5)$$

In the equation, $\rho = Q^{1/3}/R$.

Cross and multiply the left and right ends of the upper and lower equations to obtain

$$f(\alpha) = \left(\sum_{i=1}^n V_i \rho_i^\alpha \right) \left(\sum_{i=1}^n \rho_i^{2\alpha} \ln \rho_i \right) - \left(\sum_{i=1}^n V_i \rho_i^\alpha \ln \rho_i \right) \left(\sum_{i=1}^n \rho_i^{2\alpha} \right) = 0. \quad (6)$$

After selecting the initial value and error level using Newton's iteration method, the roots can be solved after multiple iterations.

3.3.2. Attenuation Law of Vibration Velocity of Cut Hole Blasting. Nonlinear regression fitting on the horizontal radial velocity [24], horizontal tangential velocity, and vertical velocity of 21 sets of vibration data of the cut hole are performed, and the attenuation formulas with proportional distance are obtain. The fitting results are shown in Figure 3.

For the vibration caused by cut blasting, the vertical vibration speed is significantly greater than the horizontal vibration speed, and the difference between the horizontal radial vibration speed and the horizontal tangential vibration speed is not much. With the increase of proportional distance, the vertical vibration speed gradually approaches the horizontal vibration speed.

According to Figure 4, it can be concluded that the K value of the fitting curve of the vertical peak vibration velocity of the cut hole is greater than that in the horizontal direction, which indicates that the vertical vibration velocity carries a large amount of energy to a certain extent. The

attenuation coefficient α of the vertical direction is smaller than that of the horizontal direction, indicating that the attenuation speed of vertical vibration velocity is relatively slower.

4. Electronic Detonator Interference and Vibration Reduction Test

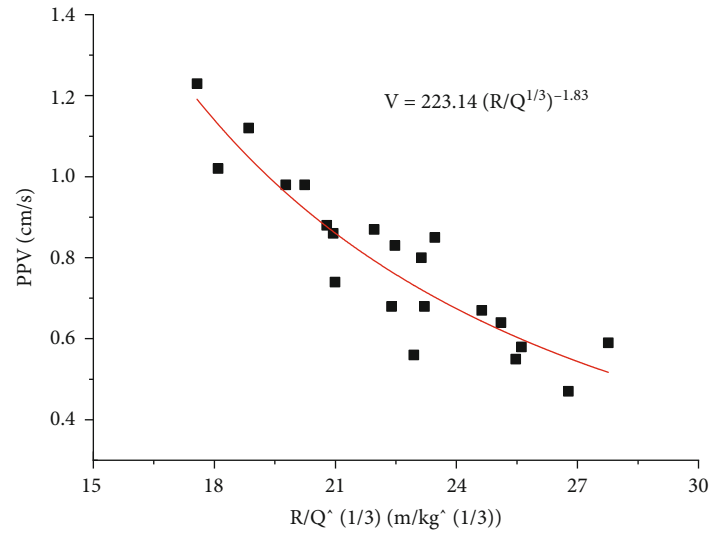
Excessive vibration velocities caused by blasting excavation in mountain tunnels will affect the stability of surrounding rock [25–27]. Therefore, effective vibration reduction measures are need to be taken to reduce the influence of blasting vibration on the primary lining and the secondary lining. Conventional measures for reducing tunnel blasting vibration usually include reducing the total charge or restricting the charge of a single section and selecting lower-power explosives and uncoupled charges [28–32]. These measures can produce a certain effect. However, in actual applications, they will increase the cost of engineering progress. Vibration reduction through delay setting is also one of the common measures to reduce vibration, but nonelectric millisecond detonators have large errors, and their accuracy is difficult to meet the time requirements of the delay interval. But for electronic detonators, they can be set freely through electronic chips, which make it possible to reduce the effect of blasting vibration through interference reduction.

4.1. Single-Hole Blasting Test. Obtaining the vibration waveform and main vibration period of the single-hole blasting is necessary for realizing interference and vibration reduction. There are many factors influencing the frequency of blasting vibration, but cannot be accurately obtained by calculation. It is the easiest and most convenient method to monitor the blasting vibration waveform at the vibration reduction point from the single-hole blasting test, and the main vibration period and waveform can be read from the vibration waveform measured on site.

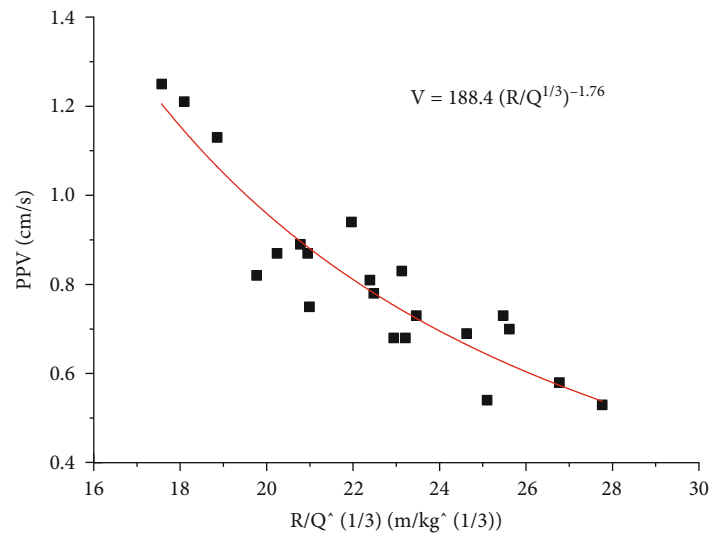
It is known from previous tunnel blasting tests that the peak vibration velocity generated by the cut hole is the largest; therefore, optimizing the delay time of the cut hole is the key to achieve vibration reduction. In order to obtain a complete single-hole waveform without superimposing other interference waveforms, a test hole is set in the middle of the cut area, and the delay time between the test hole and the entire blasting network is set to be 100 ms. The layout of the test holes is shown in Figure 4. The charge of the test holes is consistent with the single hole of conventional cut hole, and the charge is 2.1 kg. The measuring points are arranged at the bottom of the tunnel section with a burst center distance of 40 m. The arrangement of test holes in the cut area is shown in Figure 5.

The single-hole vibration waveform is obtained in the single-hole blasting test, and the velocity-time history curve of the typical single-hole blasting waveform collected by the vibration measuring points is shown in Figure 6.

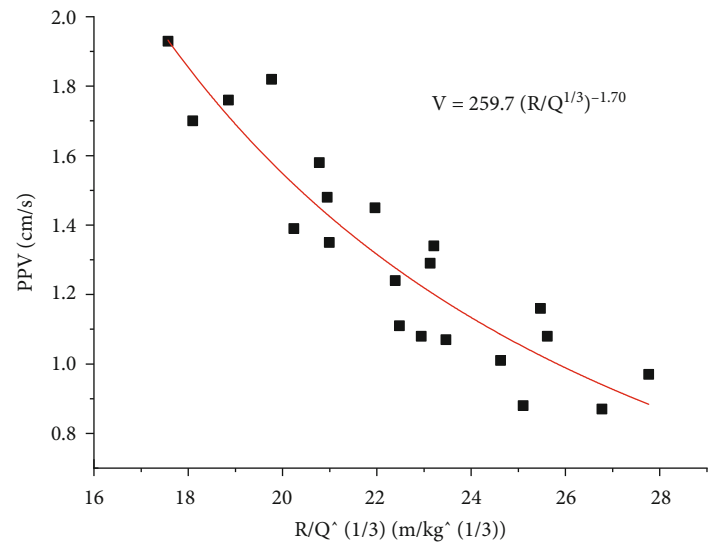
From Figure 6, it can be seen intuitively that the single-hole blasting often only has a pair of main wave peaks and valleys, and the maximum vibration generally appears at the first wave peak or valley. In addition, the first wave peak



(a) Horizontal radial direction



(b) Horizontal tangential direction



(c) Vertical direction

FIGURE 4: Vibration fitting curve of Cut hole blasting floor.

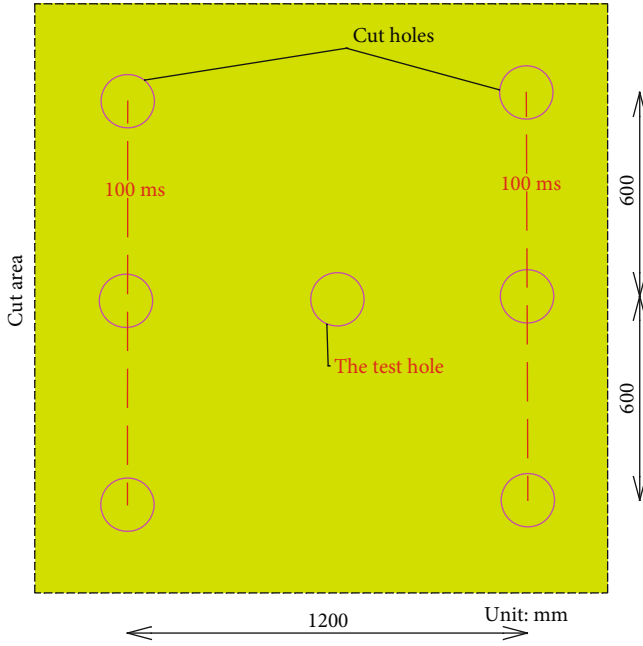


FIGURE 5: Arrangement of test holes in the cut area.

appears at 20.3 ms, with a peak vibration velocity of 0.297 cm/s, followed by a trough at 32.4 ms, with a vibration velocity of -0.354 cm/s. The 12.1 ms time from the appearance of the wave crest to the disappearance of the wave trough is the main vibration phase of the single-hole blasting waveform, and the duration of the entire vibration does not exceed 65 ms.

4.2. Superposition Prediction of Blasting Test Based on Measured Single Hole Vibration Waveform

4.2.1. Realization of Interference and Vibration Reduction by Electronic Detonator. The interference reduction method based on the measured blasting vibration signal separates the single-hole waveform (or subsignal) from the recorded short-distance blasting vibration signal and then analyzes the single-hole waveform in different delays. The superposition result under time is used to optimize the delay time of the slight difference, so as to achieve the purpose of interference and vibration reduction, and realize the active control of the blasting vibration disaster. The specific steps are as follows:

- (1) Using signal interception technology for signal processing, the single-hole waveform signal which appears is extracted from the total signal (that is, the measured blasting vibration signal)
- (2) Based on the MATLAB program platform, the single-hole waveform under different delays is superimposed, and the number of superimpositions is determined by the number of on-site holes. In this experiment, the number of cuts $N = 6$; thus, the number of superimpositions is 5

- (3) Count the maximum peak vibration velocity after superimposing each delay, and take the delay used by the minimum peak vibration velocity as the optimal differential delay time

For the superimposition operation of blasting vibration signals in MATLAB, the following assumptions are required: the single-hole vibration waveform generated by each blast-hole is basically the same; the time and frequency characteristics of each vibration wave on the different propagation path are unchanged; The delay time of the electronic detonator is equal to the time of the misaligned waveform addition. Under the premise of the above assumptions, the vibration propagation is regarded as a linear system meeting the engineering requirements [32, 33].

Take the collected single-hole blasting vibration waveform as the fundamental wave [34], and the single-hole waveforms with different delay times are shifted by a certain time interval and then added to determine the delay time which minimizes the peak vibration speed of the vibration signal and the best superposition effect [35].

4.2.2. Realization of the Superposition of Single-Hole Vibration Waveform in MATLAB. In this test, the analysis of the vibration monitoring results shows that the vibration caused by the cut blasting is the largest; thus, the cut area is the focus of the entire vibration reduction process [36].

There are a total of 6 cut holes in the face of the upper step, which arranged in two rows. Based on the measured single-hole vibration waveform and the principle of linear superposition of vibration signals, the additive predicted waveforms under different delay times are obtained. The single-hole vibration waveform collected by the TC-4850 vibrometer is input to MATLAB software, and the single-hole waveform is drawn. There are 6 cut holes; thus, the number of times stacking selected for each stacking operation in the stacking operation is $N = 5$. In this way, the superimposed waveforms generated by the sequential blasting of 6 blastholes in the cut area under different delay times can be obtained.

4.2.3. Peak Vibration Velocity Characteristics of the Blasthole Superimposed Signal in the Cut Area. With the help of the for-loop program in MATLAB software, the repeated superposition of single-hole waveforms can be realized. After changing the delay time, through multiple program loop calculations and graphs, a total of 50 superimposed cut blasting waveforms are obtained from $\Delta T = 0 \sim 50$ ms. Due to the limitation of the length of the article, only the representative superimposed waveforms at the delay time of 0 ms, 7 ms, and 12 ms are listed below. The typical superimposed waveforms are shown in Figure 7.

The single-hole blasting vibration waves are superimposed with different micro-difference time, and the numerical increment of repeated superposition is $\Delta = 1$ ms, so as to draw the positive and negative velocity peaks of single-hole blasting waveform superimposed. According to Figure 7(c) of the superimposed result under the delay time of 12 ms, it can be seen that when the delay interval is

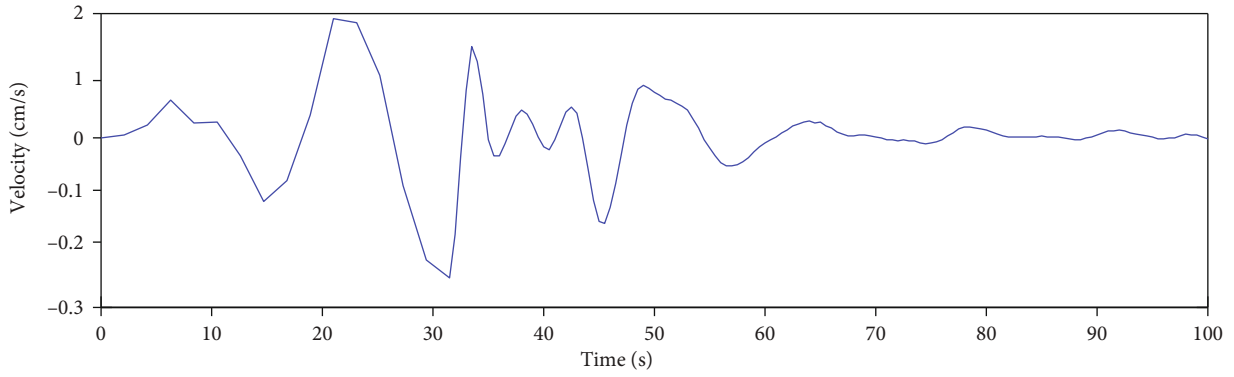
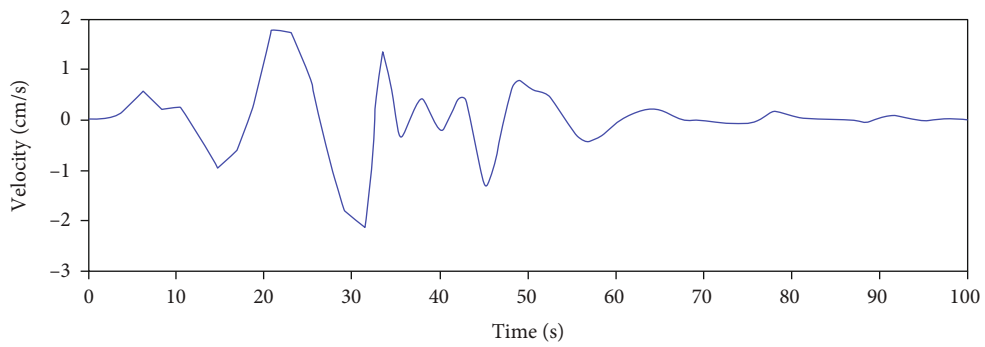
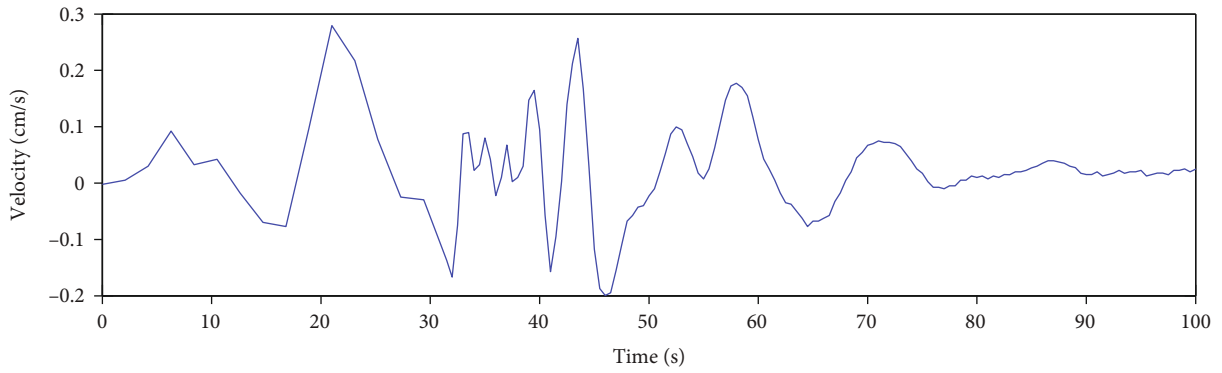


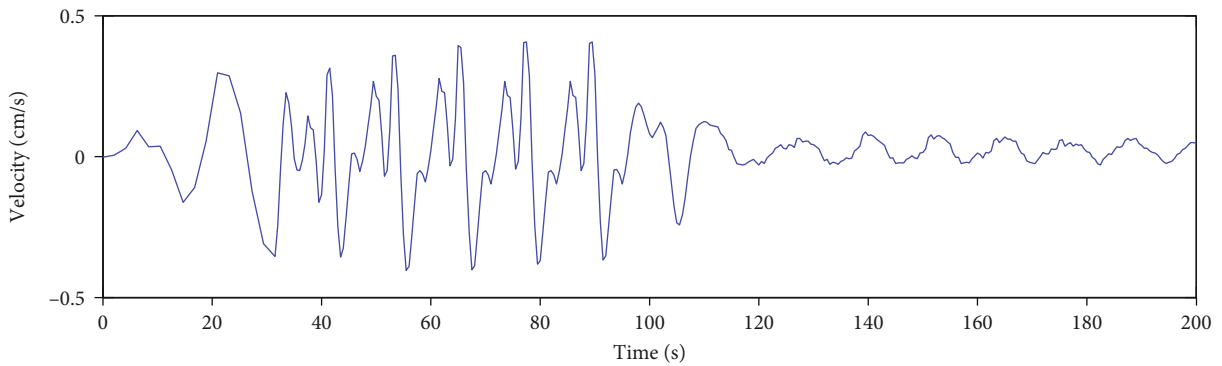
FIGURE 6: Vibration waveform of single hole blasting.



(a) Superposition vibration waveform of single hole with delay of 0 ms



(b) Superposition vibration waveform of single hole with 7-ms delay



(c) Superposition vibration waveform of single hole with 12-ms delay

FIGURE 7: Superposition vibration waveform under different delay time.

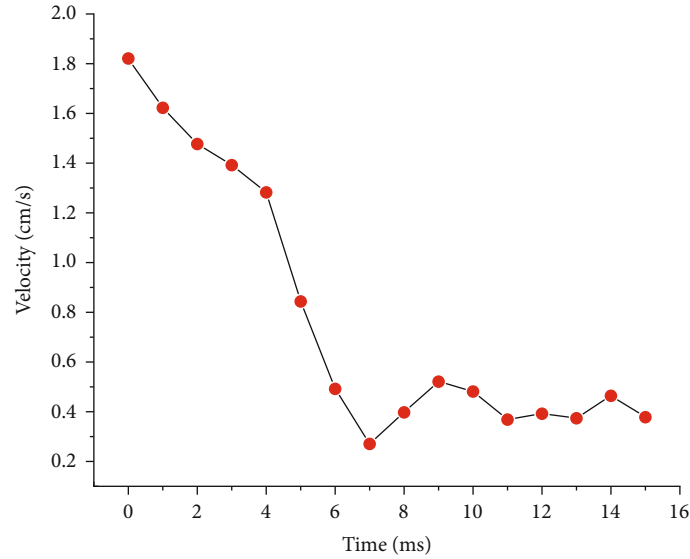


FIGURE 8: Positive peak vibration velocity diagram after superposition of different micro-difference waveforms.

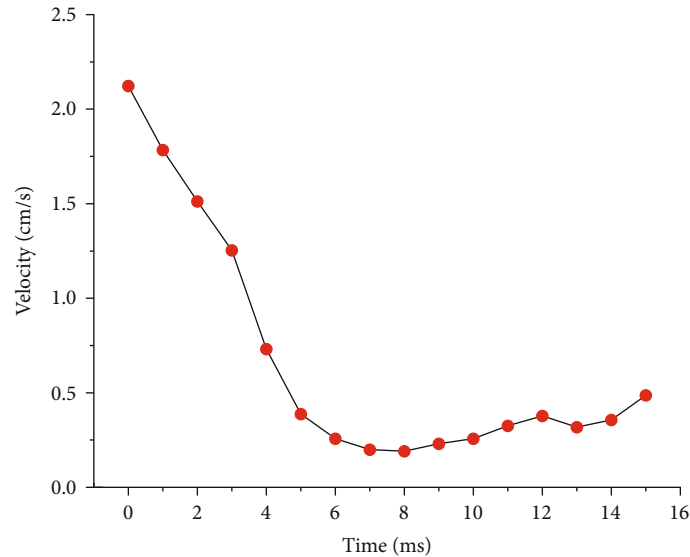


FIGURE 9: Negative peak vibration velocity after superposition of different millisecond waveforms.

greater than $\Delta T = 12$ ms, the main vibration phase of the adjacent blasting vibration waveform does not superposition. As the delay interval is too large, it is not conducive to the rock breaking effect. Therefore, only the superimposed waveforms with an interval of $\Delta T = 0 \sim 15$ ms are analyzed in the following. A set of delay times will be obtained for each Δt by the for-loop program. For the superimposed waveform diagrams, the positive peak vibration velocity and negative peak vibration velocity in each group of waveform diagrams are abstracted. For the convenience of observation, the law of the positive peak vibration velocity and negative peak vibration velocity with the delay time is drawn in Figures 8–9.

In order to analyze the calculated results, the positive and negative peak vibration velocities of the superimposed waveforms are plotted separately in Figures 8–9:

- (1) On the whole, the maximum peak vibration velocity of the single-hole waveform superimposition appears in the superimposed waveform with the delay time of 0 ms, and the peak vibration velocity caused by the maximum amount of the segment charge is the largest. Figure 7(a) shows the superimposed vibration waveform under the delay time of 0 ms. It can be seen that the positive peak vibration velocity is 1.8 cm/s, which is about 6 times the value of the positive peak vibration speed of single-hole blasting
- (2) With the increase of differential time, the positive peak vibration velocity of the waveform after superposition shows a decreasing tendency. The attenuation speed of superimposed vibration velocity is relatively slow within $\Delta T = 0 \sim 4$ ms, but when $\Delta T = 4 \sim 7$ ms, the attenuation acceleration

TABLE 2: Vibration reduction rate under different delay time intervals.

Delay time (ms)	Positive peak vibration (cm/s)	Negative peak vibration velocity (cm/s)	Positive vibration reduction rate	Negative vibration reduction rate
0	1.820	2.122	0	0
1	1.623	1.906	10.82%	10.18%
2	1.477	1.545	18.85%	27.19%
3	1.392	1.484	23.52%	30.07%
4	1.283	1.359	29.51%	35.96%
5	0.844	0.898	53.63%	57.68%
6	0.493	0.458	72.91%	78.42%
7	0.271	0.199	85.11%	90.62%
8	0.398	0.191	78.13%	91.00%
9	0.521	0.231	71.37%	89.11%
10	0.482	0.258	73.52%	87.84%
11	0.369	0.325	79.73%	84.68%
12	0.392	0.378	78.46%	82.19%
13	0.374	0.318	79.45%	85.01%
14	0.464	0.356	74.51%	83.22%
15	0.378	0.487	79.23%	77.05%

becomes almost linear, and the vibration speed is significantly reduced. During this interval, the main vibration phases of the front and back waveforms are superimposed. When $\Delta T = 7$ ms, the positive peak vibration velocity of the waveform after superposition is 0.271 cm/s, which is even lower than the peak vibration velocity produced in the single-hole blasting. At this time, the wave peak generated by the leading wave and the trough of the following traveling wave may produce superposition and cancel, which proves that the millisecond blasting can not only reduce the charge of a single blasting, but also cause interference superposition of each vibration wave, which can achieve a good vibration reduction. The test results show that when the delay time $\Delta T = 4 \sim 7$ ms, the effect of interference reduction is the most significant, which is consistent with the delay time of interference reduction $T/3 < \Delta T < 2T/3$ determined based on theoretical calculations, and this result is verified by experiments

- (3) As ΔT further increases, the effect of interference and vibration reduction will no longer be significant. The main vibration phase of the preceding wave is no longer superimposed with the main vibration of the backward wave but is superimposed with the aftermath of the backward wave; thus, the peak amplitude of the reduction of the vibration speed is also reduced. The positive peak vibration speed of the superimposed waveform at this stage fluctuates in a small range around the positive peak vibration speed of the single-hole blasting

In the negative peak vibration velocity after the superposition of different micro-difference waveforms shown in Figure 8, it can be seen that the overall changing trend is roughly the same as that of the positive peak vibration

speed. Take the delay time to the minimum negative peak vibration speed. From Figure 8, it can be seen that at 8 ms, the minimum peak vibration velocity appears, with a value of 0.191 cm/s. The obvious vibration reduction delay interval is still in the range of $T/3 < \Delta T < 2T/3$.

In order to more intuitively reflect the superimposed vibration reduction effect of different micro-difference intervals, the vibration reduction rate r_v of the superimposed peak vibration speed can be obtained by Equation (7)

$$r_v = \frac{v_{\max} - v_i}{v_{\max}} \times 100\%, \quad (7)$$

where the v_{\max} is the velocity when two holes are detonated at the same time; v_i represents the superimposed peak vibration velocity of different micro-difference times.

The vibration reduction rate of the peak vibration velocity in the positive and negative directions is calculated by Equation (7) in Table 2. In order to show the law of the vibration reduction rate with the delay interval more intuitively, the vibration reduction rate of the positive peak vibration velocity and the negative peak vibration velocity in the table are plotted in Figure 10.

Figure 10 shows the evolution of the vibration reduction rate with the delay interval. It can be seen that the vibration reduction rate is the largest when the delay interval is 7~8 ms. As the delay interval increases, after the vibration reduction rate reaches the maximum point, there will be a decreasing trend of the fluctuations, and the vibration reduction effect will no longer be significant.

Considering the positive and negative peak vibration velocities after the superposition of different delay time comprehensively, the positive and negative peak vibration velocities reach the minimum values, respectively, when the delay time $\Delta T = 7$ ms and $\Delta T = 8$ ms, and the negative peak

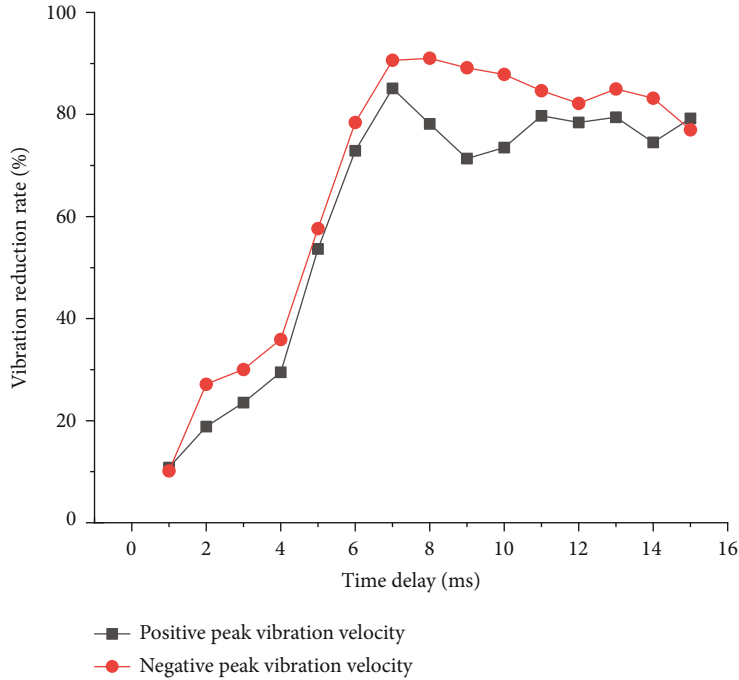


FIGURE 10: Variation of vibration reduction rate with time delay.

TABLE 3: Statistics of peak vibration velocity of the cut test.

Blasthole time delay (ms)	0	3	4	5	6	7
Peak vibration velocity of cut hole(cm/s)	2.08	0.74	0.67	0.56	0.42	0.30
Peak vibration velocity of full section(cm/s)	2.08	1.25	1.03	1.28	1.59	1.47

vibration velocities of the two delay intervals are similar, and considering the synergism of blasting and rock breaking effect, after comprehensive consideration, 7 ms is selected as the optimal vibration reduction delay interval for the cut area.

4.3. Analysis of Vibration Reduction Effect of Electronic Detonators

4.3.1. Design of Vibration Reduction Test for Group Hole Blasting. Based on the analysis of the superposition calculation of measured single-hole waveform, it is found that the best delay time for vibration reduction during single-hole continuous blasting is 7 ms, and the effect of interference reduction is the most significant within the delay interval of 3~7 ms. Next, the six blastholes in the cut hole area are sequentially set for the delay interval. When the vibration reduction test of the step cut in the tunnel is performed, the typical delay time is selected for the test, and the cut is made during each blasting test. The initiation time of the regional blasthole is 50 ms, $50 + \Delta T$ ms, $50 + 2\Delta T$ ms, $50 + 3\Delta T$ ms, $50 + 4\Delta T$ ms, and $50 + 5\Delta T$ ms, respectively, and in the area blasting test, ΔT of the 5 cuts is taken 3~7 ms in sequence.

In order to compare with the vibration waveform formed by the simultaneous blasting of the cut hole, during the cut test, the burst center distances of the vibration data

collection points with different delay times are consistent with the simultaneous blasting test, and the distance between the measuring points is set at 40 m from the face of the tunnel.

4.3.2. Analysis of Vibration Velocity of Blasting Vibration Reduction. After 5 times of the cut vibration reduction tests under different delay intervals, a total of 5 sets of blasting vibration waveforms are obtained. By using MATLAB, the vibration waveform of the upper step is intercepted, and only that of the upper step is used for analyzing. Through observation, it is found that the vibration waveform caused by the blasting of the upper step is significantly lengthened, and the vibration velocity of the cut is changed from a large peak to a vibration waveform composed of several small peaks. From the perspective of the entire vibration waveform, it can be seen that the peak vibration velocity during the up-step blasting process is generated in the cut area but in the peripheral hole area with the largest single-stage charge. The blasting of cut holes and caving holes creates a good free surface for peripheral hole blasting. Therefore, the vibration caused by the surrounding hole blasting is relatively limited. This method of continuous initiation of the cut hole achieves a good vibration reduction effect.

During the cut test, the burst center distance of the measuring point was maintained at 40 m, the total charge of the upper step does not change much, and the charge of the cut

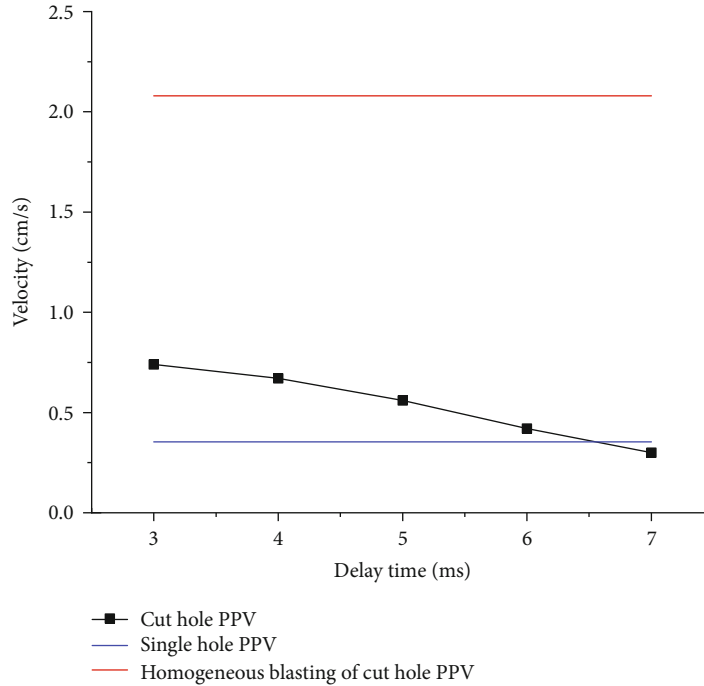


FIGURE 11: Statistics of blasting peak vibration velocity in cut area under different delay time.

hole in the cut area remained the same. According to the vibration waveform of the monitored tunnel, the peak vibration data were sorted and analyzed, and the Z (vertical) peak vibration velocity of the vibration wave measured by the blasting is obtained, as shown in Table 3 and Figure 10.

It can be seen from Figure 11 that the blasting vibration law of the measured vibration velocity of the blasting area under different delay times is consistent with the change law obtained by the MATLAB superposition operation. The most significant delay period for interference reduction is 3~7 ms. During this interval, the maximum peak vibration velocity in the cut area is far less than the peak vibration velocity generated when the 6 cut holes burst together. When the delay is 7 ms, the peak vibration velocity generated is even lower than that generated by single-hole blasting. This fully shows that the millisecond blasting not only reduces the vibration by reducing the single-stage charge, but also causes the superposition and cancelation of the vibration waveforms. The vibration velocity is even lower than that of the single-hole blasting.

5. Conclusions

Based on the vibration monitoring results of Xiaoxiku tunnel, using the nonlinear regression method and MATLAB software, this paper studies the nonlinear regression analysis of typical waveform and vibration velocity of blasting vibration, regression parameters, and waveform superposition. The main conclusions obtained are as follows:

- (1) It is found that the vertical vibration velocities are much greater than the horizontal radial and horizontal tangential vibration velocities, as the proportional

distance increases. The vertical vibration velocity is gradually approaching the horizontal radial and horizontal tangential vibration velocity, but within the range of the measured proportional distance, the horizontal radial and horizontal tangential vibration velocity are always less than the vertical vibration velocity. The vibration speed caused by the slot is the largest

- (2) From the analysis of the fitting parameters K and α value, the K value of the peripheral hole is smaller than that of the cut hole as a whole, and the α values of the three vibration velocity directions of the cut hole and the peripheral hole are not much different. Compared with the horizontal direction, the vertical vibration speed of the measuring points is the largest, and the attenuation speed is the slowest
- (3) Through the single-hole blasting field test, the single-hole blasting vibration waveform is obtained. It was found that the main vibration period of single-hole blasting is $T = 12.1\text{ms}$, and the measured single-hole wave has only a pair of main peaks and valleys, followed by a small after-vibration, and the maximum value of the vibration appears at the trough of the main vibration phase, with the vibration speed of -0.354cm/s
- (4) Based on the MATLAB program platform, the misalignment and superposition operation of the single-hole vibration signal was performed on the 6 blastholes in the cut area, and the vibrations of the 15 single-hole waveforms were obtained under the delay time $\Delta T = 0 \sim 15\text{ms}$. After statistics of their

respective peak vibration speeds, it is found that the superimposed vibration speed appears the maximum value under $\Delta T = 0\text{ms}$, and the effect of interference reduction in $\Delta T = 4 \sim 7\text{ms}$ is significant. The vibration reduction effect is the best under $\Delta T = 7\text{ms}$, in which the superimposed overall waveform is relatively uniform, and the vibration duration is moderate. After comprehensive consideration, $\Delta T = 7\text{ms}$ is determined as the best delay time

Data Availability

The data to support the findings of this study are included in the article.

Conflicts of Interest

There is no conflict of interest in this study.

Acknowledgments

The author's research work was supported by the National Natural Science Foundation of 403 China (No. 520640251, No. 52164009, and No. 52164010).

References

- [1] H. Kairong, "State-of-art and prospect of tunnels and underground works in China," *Tunnel Construction*, vol. 35, no. 2, pp. 95–107, 2015.
- [2] R. Holmeberg and P. Persson, "Design of tunnel perimeter blasthole patterns to prevent rock damage," *Institution of Mining & Metallurgy*, vol. 89, no. 6, pp. 27–32, 1980.
- [3] Z. X. Yan and W. U. Wu, "The study of blast vibration effect and safety," *Rock and Soil Mechanics*, vol. 2, pp. 201–203, 2002.
- [4] B. Liu, S. Yu, and Z. Chu, "Time-dependent safety of lining structures of circular tunnels in weak rock strata," *International Journal of Mining Science and Technology*, vol. 32, no. 2, pp. 323–334, 2022.
- [5] J. Ma, X. L. Li, J. G. Wang et al., "Experimental study on vibration reduction technology of hole-by-hole presplitting blasting," *Geofluids*, vol. 2021, Article ID 5403969, 10 pages, 2021.
- [6] J. Wang, T. Zuo, X. Li, Z. Tao, and J. Ma, "Study on the fractal characteristics of the pomegranate biotite schist under impact loading," *Geofluids*, vol. 2021, Article ID 1570160, 8 pages, 2021.
- [7] H. L. Fei, Z. D. Wang, and A. J. Jiang, "Study on influence of blasting vibration on ground of Metro Tunnel," *Blasting*, vol. 35, no. 3, pp. 68–73, 2018.
- [8] Z. Chao, "Research on the response law of surface particle for shallow buried tunnel blasting vibration," *Highway*, vol. 61, no. 10, pp. 246–250, 2016.
- [9] J. C. Zhang, X. J. Cao, S. Y. Zheng, and X. B. Guo, "Experimental study on vibration effects of ground due to shallow tunnel blasting," *Chinese Journal of Rock Mechanics and Engineering*, vol. 24, no. 22, pp. 4158–4163, 2005.
- [10] T. H. Ling, F. Cao, S. Zhang, L. Zhang, and D. P. Gu, "Blast vibration characteristics of transition segment of a branch tunnel," *Journal of Vibration and Shock*, vol. 37, no. 2, pp. 43–50, 2018.
- [11] H. X. Fu, Y. Zhao, J. Xie, and Y. B. Hou, "Study of blasting vibration test of area near tunnelblasting source," *Chinese Journal of Rock Mechanics and Engineering*, vol. 30, no. 2, pp. 335–340, 2011.
- [12] W. B. Lu, H. B. Li, M. Chen, C. B. Zhou, and X. X. Wu, "Safety criteria of blasting vibration in hydropower engineering and several key problems in their application," *Chinese Journal of Rock Mechanics and Engineering*, vol. 28, no. 8, pp. 1513–1520, 2009.
- [13] Y. Lu, H. Hao, G. Ma, and Y. Zhou, "Simulation of structural response under high-frequency ground excitation," *Earthquake Engineering & Structural Dynamics*, vol. 30, no. 3, pp. 307–325, 2001.
- [14] A. Bayraktar, T. Türker, A. C. Altunişik, and B. Sevim, "Evaluation of blast effects on reinforced concrete buildings considering operational modal analysis results," *Soil Dynamics and Earthquake Engineering*, vol. 30, no. 5, pp. 310–319, 2010.
- [15] U. Langefors and B. Kihlstrom, *Modern technique of rock blasting*, Halsted Press, New York, 1978.
- [16] A. B. Andrews, "Design criteria for blasting," *Proceeding of Seventh Conference on Explosives and Blasting Techniques*, pp. 173–192, 1980.
- [17] S. R. Winzer, W. Furth, and A. Ritter, "Initiator firing times and their relationship to blasting performance," in *Paper presented at the 20th U.S. Symposium on Rock Mechanics (USRMS)*, pp. P53–P66, Austin, Texas, 1979.
- [18] O. R. Bergmann, F. C. Wu, and J. W. Edl, "Model rock blasting measures effect of delays and hole patterns on rock fragmentation," *International Journal of Rock Mechanics and Mining Sciences & Geomechanics Abstracts*, vol. 11, no. 11, 1974.
- [19] Y. Nianhua, "Blasting experimental study on vibration reduction through interference waveform caused by electronic detonator," *Engineering Blasting*, vol. 19, no. 6, pp. 41–45, 2013.
- [20] L. I. Bin Feng, "Analysis of controlling measurement and blasting vibration effect," *Blasting*, vol. 2, pp. 83–85, 2003.
- [21] C. L. Zhang and K. S. Liang, "Analysis of effect of shock-absorption in presplit blasting," *Blasting*, vol. 2, pp. 17–19, 2003.
- [22] M. Gong, C. F. Shi, and X. D. Wu, "Delay time of electronic detonators based on superposition and frequency spectral analysis," *Journal of Vibration and Shock*, vol. 38, no. 15, pp. 134–141, 2019.
- [23] F. Hongxian, K. Heng, and W. Jinke, "Controlled technology of tunnel blasting in complex environment," *China Civil Engineering Journal*, vol. 50, Supplement 2, pp. 286–291, 2017.
- [24] A. I. Lawal, S. Kwon, O. S. Hammed, and M. A. Idris, "Blast-induced ground vibration prediction in granite quarries: An application of gene expression programming, ANFIS, and sine cosine algorithm optimized ANN," *International Journal of Mining Science and Technology*, vol. 31, no. 2, pp. 265–277, 2021.
- [25] W. Hao, G. Zhao, and S. Ma, "Failure behavior of horseshoe-shaped tunnel in hard rock under high stress: phenomenon and mechanisms," *Transactions of Nonferrous Metals Society of China*, vol. 32, no. 2, pp. 639–656, 2022.
- [26] Y. Xin, P. Gou, and F. Ge, "Analysis of stability of support and surrounding rock in mining top coal of inclined coal seam," *International Journal of Mining Science and Technology*, vol. 24, no. 1, pp. 63–68, 2014.
- [27] F. Q. Gao, A. J. Hou, X. L. Yang, and J. Yang, "Analysis of blasting vibration frequency based on dimensional method," *Blasting*, vol. 27, no. 3, pp. 1–3, 2010.

- [28] X. Hong-bing, W. Hai-bo, and Z. Qi, "Comprehensive analysis of controlling technology of blasing vibration effect," *Engineering Blasting*, vol. 2, pp. 83–86, 2007.
- [29] Z. Zhi-qiang, Y. Jian-heng, and W. Bo, "Present situation and suggestions of research and development of controlled blasting technology," *Mining Research and Development*, vol. 30, pp. 103–108, 2010.
- [30] Z. Cheng-Jun, "Analysis of safety control measures for tunnel blasting construction," *Coal Mine Blasting*, vol. 37, pp. 27–31, 2019.
- [31] L. Ting-chun, S. Xiao-hu, and Z. Qiang, "Seismic effect of high slope under the action of blasting load and research on blasting vibration reduction methods," *Blasting*, vol. 37, pp. 27–31, 2019.
- [32] Y.-P. Zhang, X.-B. Li, G.-Y. Zhao, Y.-J. Zuo, and W.-H. Wang, "Time-frequency analysis of blasting vibration signals," *Chinese Journal of Geotechnical Engineering*, vol. 12, pp. 1472–1477, 2005.
- [33] Y. G. Zhang, J. Tang, Y. M. Cheng et al., "Prediction of landslide displacement with dynamic features using intelligent approaches," *International Journal of Mining Science and Technology*, vol. 2, no. 1, pp. 1–11, 2022.
- [34] L. Dong, Q. Tao, H. Qingchun et al., "Acoustic emission source location method and experimental verification for structures containing unknown empty areas," *International Journal of Mining Science and Technology*, 2022.
- [35] S. Li, Y. G. Zhang, M. Y. Cao, and Z. N. Wang, "Study on excavation sequence of pilot tunnels for a rectangular tunnel using numerical simulation and field monitoring method," *Rock Mechanics and Rock Engineering*, vol. 1, pp. 1–15, 2022.
- [36] G. Han, Y. Zhou, R. Liu, Q. Tang, X. Wang, and L. Song, "Infuence of surface roughness on shear behaviors of rock joints under constant normal load and stiffness boundary conditions," *Natural Hazards*, vol. 2, pp. 1–18, 2022.